Microstructure and Nonlinear Properties of Microwave-Sintered ZnO–V$_2$O$_5$ Varistors: II, Effect of Mn$_3$O$_4$ Doping

Cheng-Tzu Kuo, Chang-Shun Chen,[†] and I-Nan Lin[‡]

Institute of Materials Science and Engineering, National Chiao-Tung University, Hsinchu,
Taiwan 300, Republic of China

The microstructure and nonlinear current–voltage characteristics of Mn$_3$O$_4$-doped ZnO–V$_2$O$_5$ ceramics, microwave-sintered at 800°–1200°C for 10 min, have been investigated. A high density (96% of the theoretical density) has been achieved. The incorporation of Mn$_3$O$_4$ additives does not significantly alter the densification behavior of the ZnO–V$_2$O$_5$ materials, but rather pronouncedly increases the nonlinear coefficient ($\alpha = 23.5$) and markedly suppresses their leakage current density ($J_L = 2.4 \times 10^{-6}$ A/cm^2). On the other hand, the intrinsic properties of the materials, including the Schottky barrier height (Φ_b) and the donor density (N_d), are only moderately modified; that is, $\Phi_b = 1.16$ eV and $N_d = 5.4 \times 10^{17}$/cm^3. X-ray diffractometry analyses and energy-dispersive X-ray microanalyses (via scanning electron microscopy) indicate that the V$_2$O$_5$ species facilitate the densification and the development of microstructure via the formation of a liquid phase (Zn$_3$(VO$_4$)$_2$) along the grain boundaries, whereas the Mn$_3$O$_4$ species markedly enhance the nonohmic behavior of the ZnO–V$_2$O$_5$ materials by forming the surface states along the grain boundaries.

I.   Introduction

ZINC OXIDE (ZnO) materials are important *n*-type semiconductors; they are used as varistor materials, because of their highly nonohmic behavior in current–voltage (*I*–*V*) characteristics with an excellent capability of withstanding surges.[1–5] Therefore, ZnO-based varistors are extensively used as transient surge suppressors against dangerous abnormal high voltage surges, to protect electronic circuits.[6–11] It is believed that the nonlinear *I*–*V* characteristics of these materials result from the grain-boundary layer, which is essentially formed by a segregation of large ionic additives, such as Bi$_2$O$_3$, Pr$_6$O$_{11}$, and BaO, at the grain boundary.[12–16] These ''varistor-forming'' ingredients affect the electrical properties and the densification behavior and microstructure evolution of ZnO ceramics. Furthermore, MnO$_2$ additives are generally included to improve the nonohmic properties of ceramics by increasing the surface-state density.[17,18]

Recently, it was reported that V$_2$O$_5$ is another varistor-forming ingredient for ZnO ceramics;[19] its use results in varistor properties that are similar to those of ZnO–Bi$_2$O$_3$ ceramics. The advantage of the ZnO–V$_2$O$_5$ system is that the materials can be sintered at relatively low temperature (i.e., ~900°C) in a conventional electrical furnace. This property is important for

applications of multilayer chip components, because the material can be cofired with a silver inner electrode, which has melting point of ~961°C.

It is generally known that the microwave sintering process can densify ceramic materials at a very rapid rate;[20–23] thus, this process has been adopted in this work to prepare the ZnO–V$_2$O$_5$–Mn$_3$O$_4$ ceramics. We have conducted an extensive examination on the effect of sintering temperature and soaking time on the densification behavior of these materials. The correlation between the microstructure characteristics of the materials and their *I*–*V* and capacitance–voltage (*C*–*V*) behaviors is discussed, with an emphasis on the role of Mn$_3$O$_4$ incorporation.

II.   Experimental Procedures

High-purity ZnO varistor powders (>99.9%) were prepared. The mixtures were composed of ZnO–V$_2$O$_5$ materials that contained 0.5 mol% V$_2$O$_5$ and *x* mol% Mn$_3$O$_4$ (where *x* = 0–1.0). The mixtures were ball-milled in a plastic jar, using zirconia balls and deionized water, for 8 h. After the mixtures were filtered and dried, they were calcined at 700°C in air for 2 h, followed by pulverization in a ball mill for 8 h to a size of ~1.0 µm; the mixtures were than uniaxially pressed at 750 kgf/cm^2 into a disk 8 mm in diameter and 2 mm thick. The green pellets, which were ~60% of the theoretical density (TD = 5.675 g/cm^3) were microwave-sintered at 800°–1200°C for 5–60 min in an applicator that was made of a WR284 waveguide (Gerling Co., Modesto, CA), using a 2.45 GHz microwave generated from a commercial source (Model GL107 magnetron, Gerling). The temperature profile was measured by using a Pt–13% Rh thermocouple that was placed near the sample surface. The heating rate was controlled at 60°C/min, and the cooling rate was controlled at 145°C/min for sintering temperatures >500°C. The details of the apparatus used for the microwave sintering process are described elsewhere.[24] For comparison, the samples were also prepared via a conventional sintering process; that is, sintering at 900°–1200°C for 60 min in an electrical furnace. The heating rate and the cooling rate for this latter process each were 5°C/min.

The crystal structure and microstructure of the sintered samples were examined using X-ray diffractometry (XRD) (Model XD-5, Shimadzu Co., Kyoto, Japan) and scanning electron microscopy (SEM) (Model JSM-840A, JEOL, Tokyo, Japan), respectively. The density of sintered specimens was measured by using the Archimedes method. The average grain size ($\overline{G}$) was calculated as described by Mendelson,[25] with a multiple factor of 1.56. The *I*–*V* properties of these samples were recorded by using an electrometer (Model 237 I-V, Keithley Instruments, Cleveland, OH) in dc source after the indium–gallium (40:60) alloy was rubbed onto the sample surface to serve as electrodes. The onset electric field (E_0) was measured at a current density of 1.0 mA/cm^2, the nonlinear coefficient (α) was estimated for current-density ranges of 1.0–10 mA/cm^2, and the leakage current density (J_L) was defined as the current density at an applied field of 10 V/mm. The *C*–*V* measurements were made at room temperature using a capacitance

meter (Model HP4274A, Hewlett–Packard, Tokyo, Japan). The electrical characteristics, which include the Schottky barrier height Φ_b and the donor density N_d, were determined from the C–V data, using the model proposed by Mukae *et al.*[26]

III. Results

(1) Sintering Behavior

As reported previously, the incorporation of V_2O_5 additives markedly enhances the densification rate of the ZnO materials. Figure 1(a) shows that only 800°C (for 10 min) is required in the microwave sintering process for these materials to attain a density as high as 96.1% of the theoretical density (TD) for ZnO–0.5-mol%-V_2O_5 materials, whereas at least 900°C (for 10 min) is required to attain high density for pure ZnO materials. Increasing the sintering temperature, from 800°C to 1200°C (for 10 min), and the soaking time, from 5 min to 60 min (at 900°C), only moderately alters the densification behavior of the ZnO–V_2O_5 materials, as shown in Figs. 1(a) and (b), re-

(a)

(b)

Fig. 1. Variation of the density of ZnO–V_2O_5–Mn_3O_4 materials with (a) the microwave sintering temperature (with a soaking time of 10 min) and (b) the soaking time (microwave-sintered at 900°C).

spectively. Moreover, the incorporation of Mn_3O_4 only slightly reduces the sintered density without significantly modifying the temperature and time dependence of the sample density.

The grain-growth rate of the ZnO materials is also significantly increased because of the V_2O_5 addition. SEM examination shows that, when microwave-sintered at 900°C for 10 min, the grains of pure ZnO materials hardly grow; however, the ZnO–0.5-mol%-V_2O_5 materials have already developed a large grain size (~18.8 μm). The incorporation of an additional 0.3 mol% of Mn_3O_4 does not significantly affect the grain-growth rate of these materials. Figs. 2(a)–(d) reveal that a higher sintering temperature monotonously increases the grain size of the ZnO–V_2O_5–Mn_3O_4 samples, and Figs. 2(a), (e), and (f) further indicate that a longer soaking time also results in a larger grain size for these samples. The effect of the microwave sintering temperature and the soaking time on the grain-growth behavior of these material is more clearly illustrated in Figs. 3(a) and (b), respectively. The grain size increases markedly, from 18.8 μm to 30 μm, when the sintering temperature increases from 900°C to 1000°C or the soaking time extends from 10 min to 30 min (regime I in Fig. 3). The change in grain size is less pronounced beyond this range (regime II in Fig. 3). Their significance on the electrical properties of the ZnO materials will be discussed shortly.

On the other hand, the proportion of Mn_3O_4 additives that are incorporated into the ZnO–0.5 mol% V_2O_5 does not significantly modify the densification and grain-growth behaviors of these materials, as shown in Figs. 4(a) and (b), respectively. The density of the ZnO–V_2O_5–Mn_3O_4 materials varies in the range of 92.5%–94.5% of TD, whereas their grain size varies in the range of 15.5–21 μm for the samples that contain ~1.0 mol% Mn_3O_4 and have been microwave-sintered (ms) at 900°C for 10 min. For comparison, the characteristics of the ZnO–V_2O_5–Mn_3O_4 materials densified via the conventional furnace sintering (fs) process are also shown in Figs. 4(a) and (b); this comparison indicates that a pronouncedly longer sintering time (i.e., 60 min at 900°C) is required for the fs samples to achieve the same density as the ms samples, at 900°C for 10 min. Moreover, the resultant grain size of the fs samples (3–5 μm) is markedly smaller than that of the ms samples, which implies that grain-boundary mobility is low in the fs process but is markedly enhanced in the ms process.

The fact that the V_2O_5 additives can enhance the densification and grain-growth behaviors of the ZnO–V_2O_5 materials has been considered by the formation of a ZnO–V_2O_5 compound, i.e., $Zn_3(VO_4)_2$, which acts as a liquid-phase sintering aid at high temperature.[15,16] Such a phenomenon also has been examined in ZnO–V_2O_5–Mn_3O_4 materials via the XRD and EDAX microanalytic techniques. Typical phase constituents of these materials are represented by the XRD patterns of the microwave-sintered ZnO–V_2O_5 (0.5 mol%)–Mn_3O_4 (0.3 mol%) materials in Fig. 5(a); these XRD patterns reveal the presence of a $Zn_3(VO_4)_2$ secondary phase, in addition to the hexagonal ZnO. No secondary phase related to Mn_3O_4 is detected.

The EDAX microanalyses shown in Fig. 5(b) for 900°C (for 30 min) microwave-sintered ZnO–0.5-mol%-V_2O_5–0.3-mol%-Mn_3O_4 samples indicate that, in addition to the zinc species, the vanadium and manganese species both can be observed at the grain-boundary regions (pattern ''1'' in Fig. 5(b)), whereas only the manganese species are detectable, in addition to the main constituents (the zinc species), in the grain interior (pattern ''2'' in Fig. 5(b)). A similar phenomenon has been observed for the samples microwave-sintered at 1200°C (for 10 min), as shown in the EDAX microanalyses in Fig. 5(c), which reveals, again, that the vanadium and manganese species both are detected at the junction of the grains (pattern ''1'' in Fig. 5(c)) and only the manganese species coexist with the zinc species in the grain interior (pattern ''2'' in Fig. 5(c)). There is a clear implication that the V_2O_5 additives only reside at the grain-boundary region and will eutectically react with the ZnO
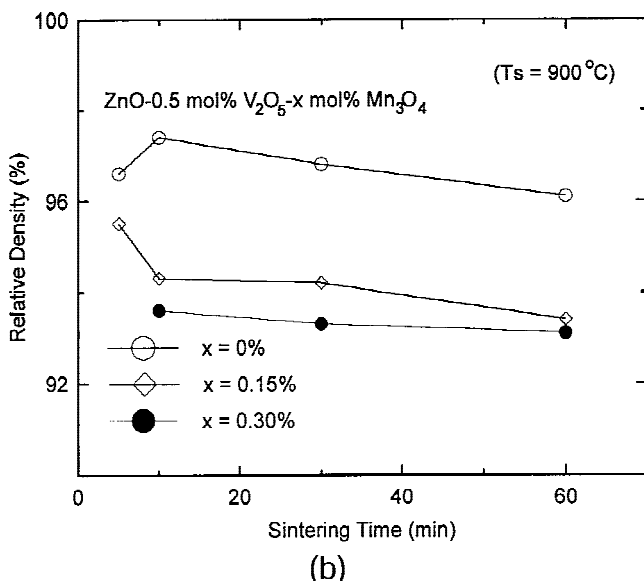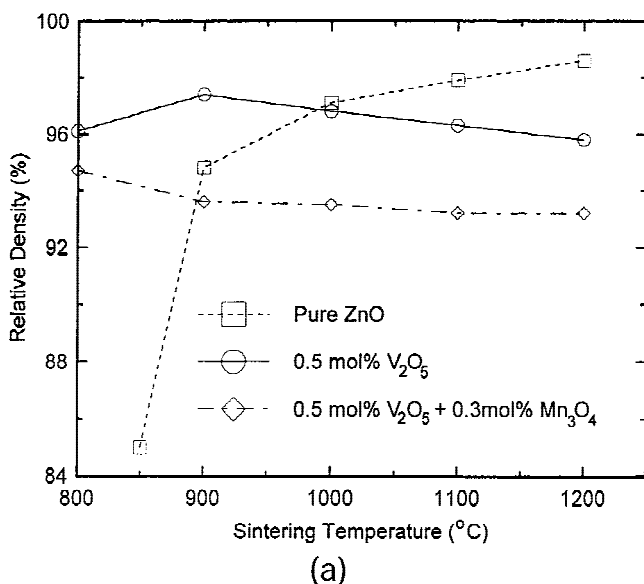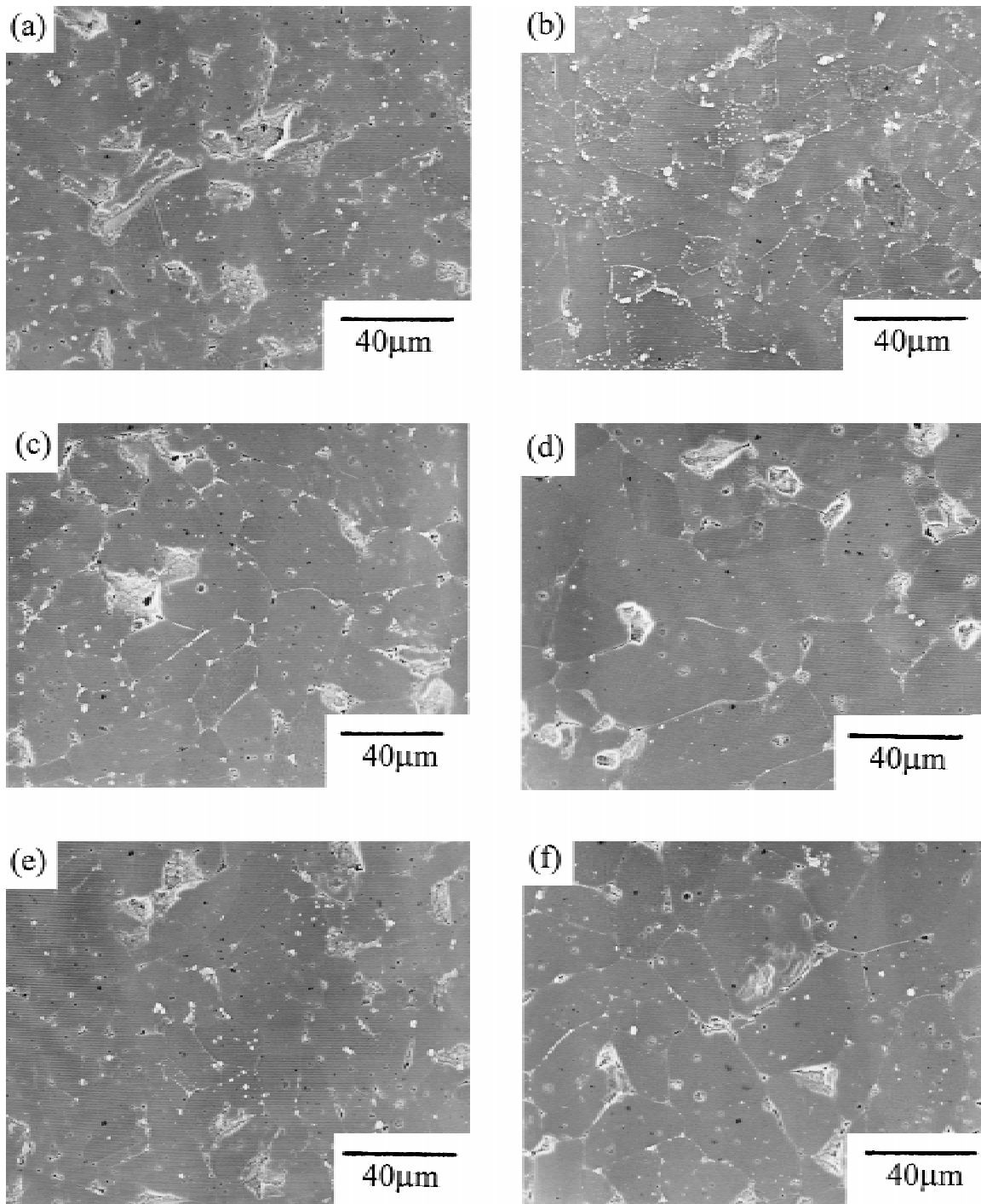
Fig. 2. SEM micrographs of the ZnO–0.5-mol%-V_2O_5–0.3-mol%-Mn_3O_4 materials microwave-sintered at (a) 900°, (b) 1000°, (c) 1100°, and (d) 1200°C for 10 min, showing the effect of sintering temperature; Figs. 2(e) and (f) are SEM micrographs of ZnO–V_2O_5–Mn_3O_4 materials microwave-sintered at 900°C for 30 and 60 min, respectively, showing the effect of soaking time.

materials in this region. This phenomenon is in agreement with the proposed model: that is, the V_2O_5 additives have enhanced the densification and grain-growth processes via the formation of a liquid phase at the sintering temperature. The significance of the phenomenon that the manganese species reside both at the grain boundaries and in the grain interior will be discussed shortly.

(2) Electrical Properties

The effect of V_2O_5 and Mn_3O_4 addition on the electrical properties of the ZnO materials has been characterized. As shown in Fig. 6(a), for the materials that have been microwave-

sintered at 900°C for 10 min, the V_2O_5 additives markedly suppress the leakage current density (J_L) of the pure ZnO materials (cf. solid and open circles in Fig. 6(a)). The incorporation of the Mn_3O_4 species further reduces the value of J_L by more than 3 orders of magnitude, which results in prominent nonohmic characteristics. For comparison, the effect of these additives on the electrical behavior of the conventionally sintered ZnO–V_2O_5–Mn_3O_4 materials (900°C for 60 min) is shown in Fig. 6(b). Generally, the furnace-sintered samples possess inferior α values, in comparison to the microwave-sintered materials, although they have smaller J_L values. These behaviors are closely related to the smaller grain size of the
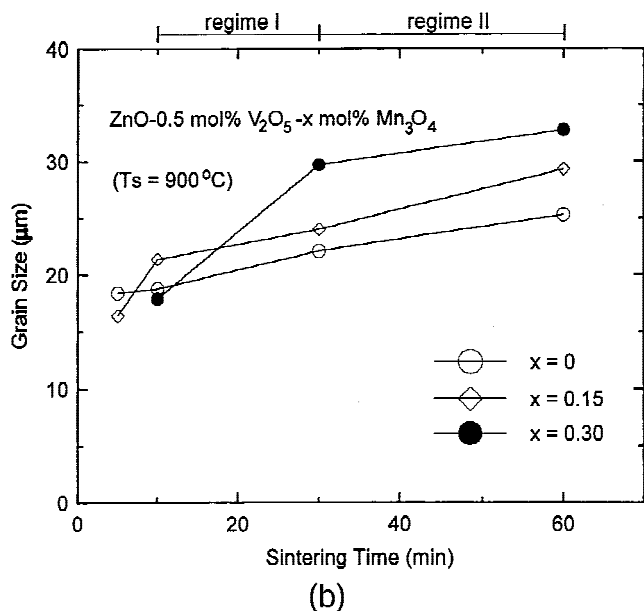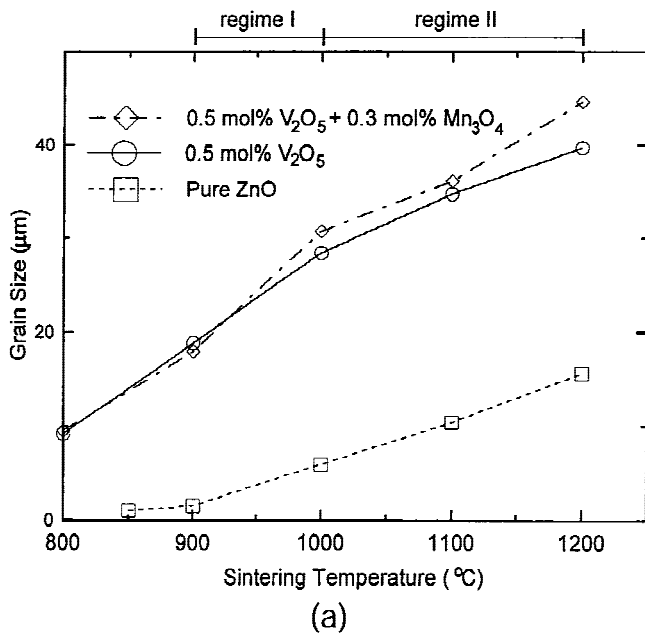
(a)

(b)

Fig. 3. Variation of the grain size of the ZnO–V$_2$O$_5$–Mn$_3$O$_4$ materials with (a) the sintering temperature (for a soaking time of 10 min) and (b) the soaking time (sintered at 900°C).
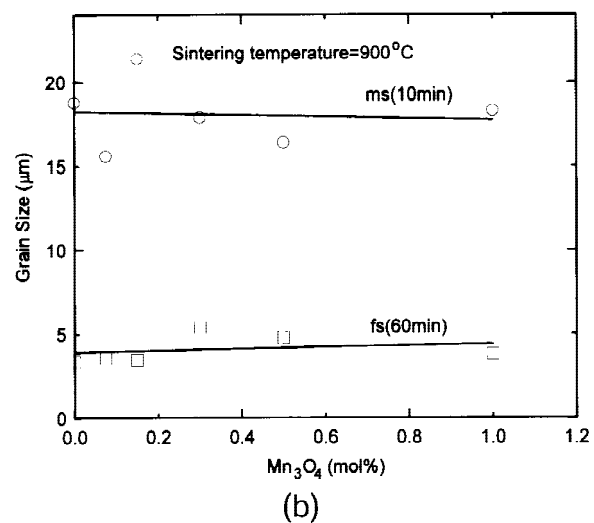

(a)

(b)

Fig. 4. Variation of (a) sintered density and (b) grain size with the Mn$_3$O$_4$ content in ZnO–V$_2$O$_5$–Mn$_3$O$_4$ materials densified by either microwave sintering at 900°C for 10 min or conventional furnace sintering for 60 min.

furnace-sintered samples (cf. Fig. 4); one can infer from this comparison that the donor additives can be fully incorporated into the grain interior of the samples only when pronounced grain-boundary migration has occurred. The advantage of the microwave sintering process over the conventional furnace sintering process in the preparation of ZnO varistor materials is, again, ascribed to the implied enhancement of the sintering process. Figure 6(b) reveals that the incorporation of Mn$_3$O$_4$ additives also significantly reduces the J_L values of the furnace-sintered samples.

To examine the effect of Mn$_3$O$_4$ doping on the electrical properties of the ZnO–V$_2$O$_5$ materials more clearly, the values of α and J_L for the samples are derived from the E–J curves that are shown in Fig. 6(a), whereas the values of Φ_b and N_d for the samples are derived from their capacitance–voltage (C^{-2}–V) characteristics (not shown). Figure 7(a) shows that J_L varies
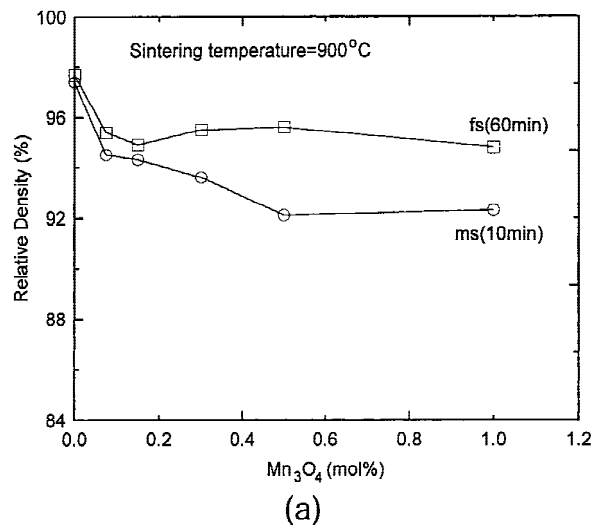
only moderately with the proportion of Mn$_3$O$_4$ additives (i.e., $J_L = 0.34 \times 10^{-5}$–$2.0 \times 10^{-5}$ A/cm^2); however, α shows a maximum value for the samples that are doped with 0.3 mol% of Mn$_3$O$_4$ (i.e., $\alpha = 17.8$). By contrast, Fig. 7(b) shows that Φ_b and N_d both possess a minimum value for the 0.3-mol%-Mn$_3$O$_4$-doped composition: that is, $\Phi_b = 0.93$ eV and $N_d = 0.8 \times 10^{18}$ cm^{-3}.

The effect of the sintering temperature and the soaking time on the electrical properties of the ZnO–0.5-mol%-V$_2$O$_5$–0.3-mol%-Mn$_3$O$_4$ materials has been examined further. The resultant E–J behaviors are shown in Figs. 8(a) and (b), respectively; these figures indicate that most of the samples possess good nonohmic properties, except for those where the microwave sintering temperature is too high (i.e., 1200°C for 10 min; see Fig. 8(a)) or the soaking time is too long (i.e., 60 min at 900°C; see Fig. 8(b)). The important electronic parameters of these materials are derived from the E–J curves and the corresponding C–V curves (not shown). The results are plotted in Figs. 9 and 10; these figures indicate that the α and J_L values are optimized for the samples sintered at 1100°C (10 min) and 900°C (30 min) (closed circles in Figs. 9 and 10). These values are as follows: $\alpha = 22$–23.5, $J_L = 1.4 \times 10^{-6}$–2.4×10^{-6} A/cm^2; $\Phi_b = 0.93$–1.21 eV, and $N_d = 0.31 \times 10^{18}$–$0.54 \times 10^{18}$
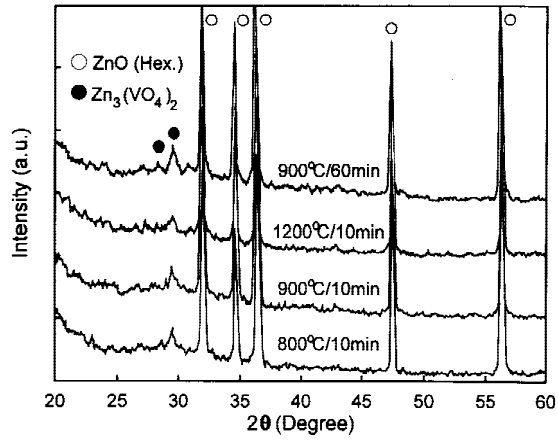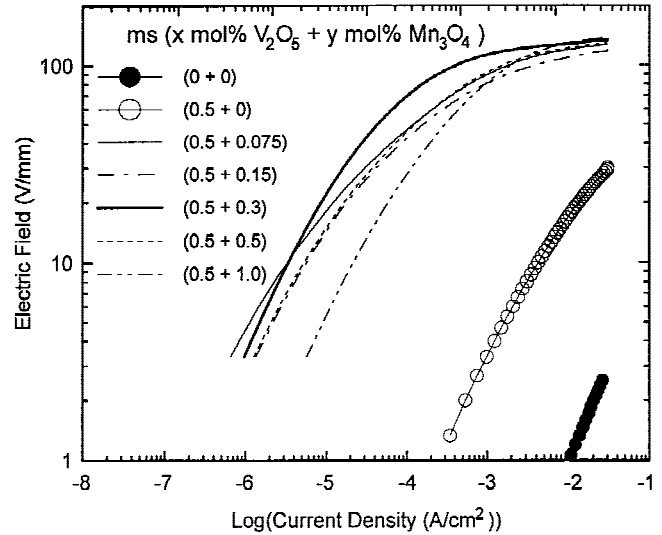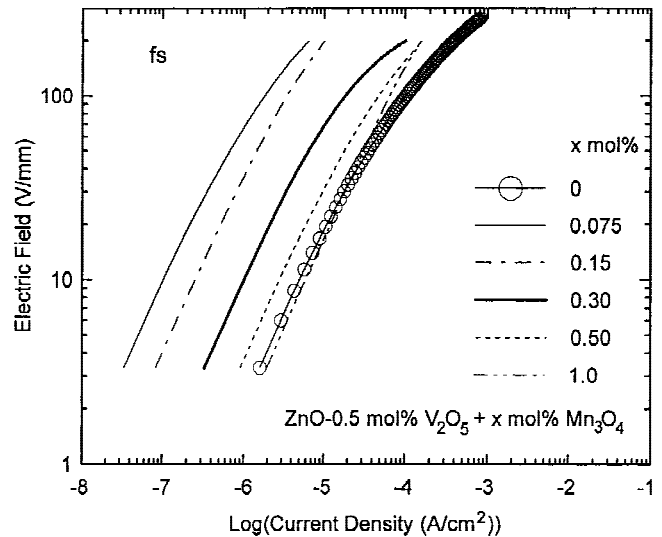
(a)
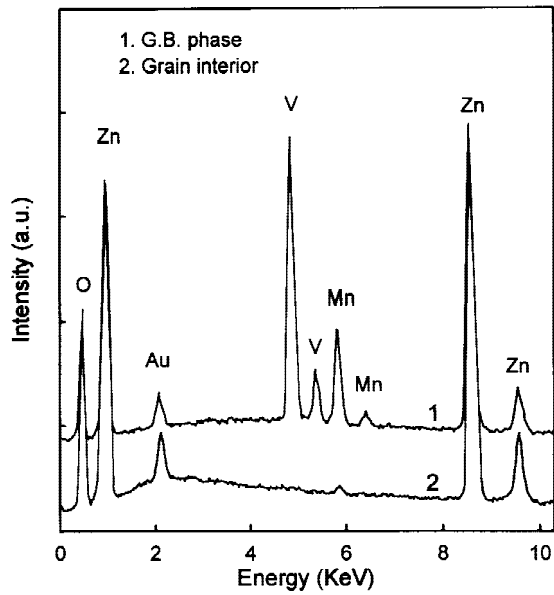
(b)
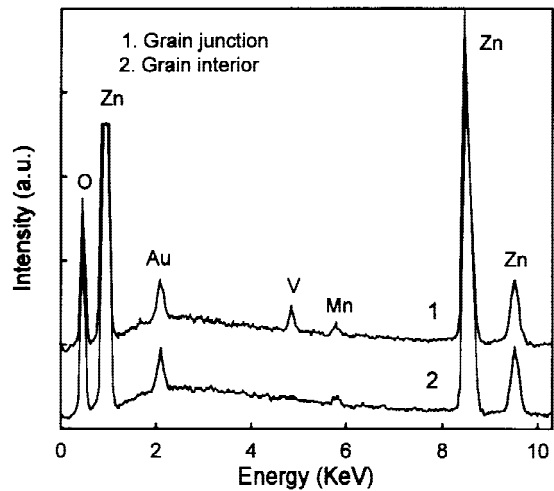
(c)

Fig. 5. (a) XRD patterns (Cu$K\alpha$) of ZnO–0.5-mol%-V₂O₅–0.3-mol%-Mn₃O₄ materials microwave-sintered at 800°–1200°C (for 10 min) or 900°C (for 60 min); Figs. 5(b) and (c) are EDAX (in SEM) patterns of the same materials microwave-sintered at 900°C for 30 min and 1200°C for 10 min, respectively.


(a)

(b)

Fig. 6. Effect of Mn₃O₄ additives on the electric-field–current-density (E–J) characteristics of the ZnO–0.5-mol%-V₂O₅ materials obtained via (a) microwave sintering at 900°C for 10 min and (b) conventional furnace sintering at 900°C for 60 min.

cm^{-3}. The nonohmic properties of the insufficiently sintered or overfired samples (open circles in Figs. 9 and 10) are inferior to those of the properly sintered samples. In other words, the processing parameters significantly affect the nonohmic properties of the ZnO–V₂O₅–Mn₃O₄ materials. Because all the samples are of high density, the modification on the nonohmic behavior of the materials is, most likely, a result of the change in the defect chemistry along their grain boundaries, which will be discussed shortly.

IV. Discussion

It is generally believed that, in the ZnO materials, the donors are the zinc species that occupy the interstitial sites of the lattice (i.e., Zn_i). The proportion of these species can be altered most easily via outward diffusion of these species via the post-annealing process. Moreover, the effective donor density (N_d) can also be reduced, because of the presence of the electron
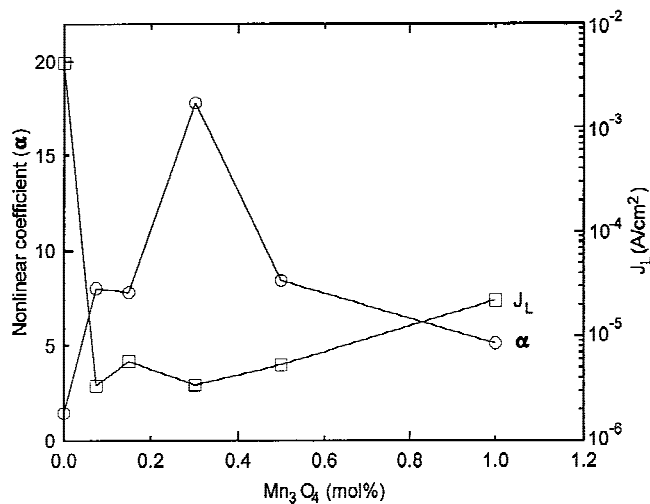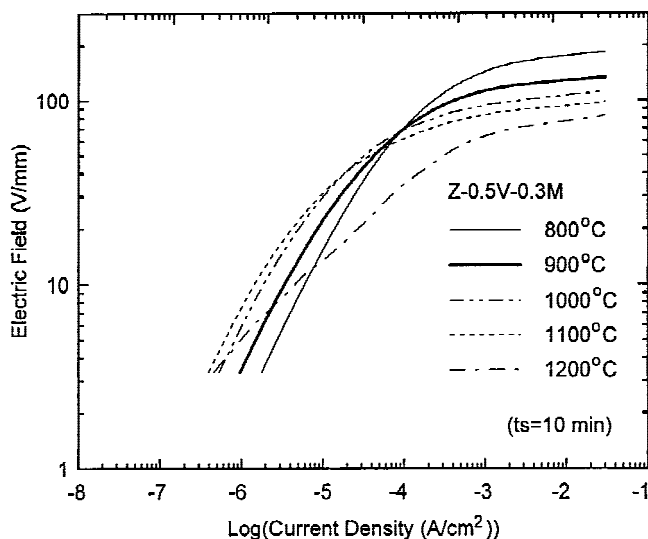
(a)
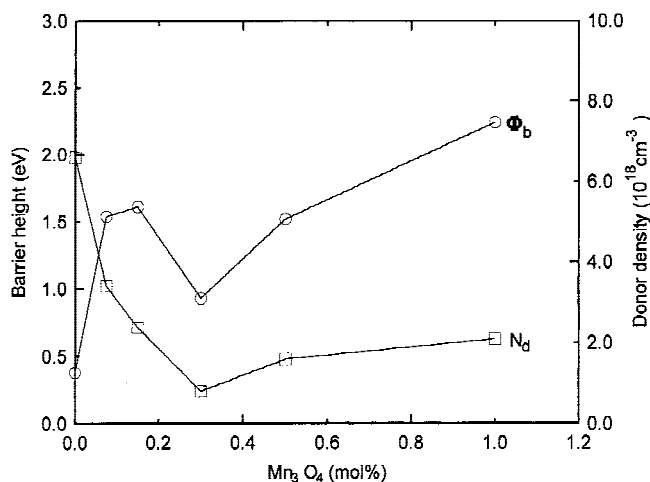
(b)

Fig. 7. Effect of Mn_3O_4 additives on various properties of the ZnO–0.5-mol%-V_2O_5 materials microwave-sintered at 900°C for 10 min ((a) (○) the nonlinear coefficient (α) and (□) the leakage current density (J_L); (b) (○) the potential barrier height (Φ_b) and (□) the donor density (N_d)).

(a)

(b)

Fig. 8. Effect of (a) the microwave sintering temperature (800°–1200°C for 10 min) and (b) the soaking time (10–60 min at 900°C) on the electrical-field–current-density (*E–J*) characteristics of ZnO–0.5-mol%-V_2O_5–0.3-mol%-Mn_3O_4 materials (the dashed curve in Fig. 8(b) represents the *E–J* characteristics of ZnO–0.5-mol%-V_2O_5 materials).
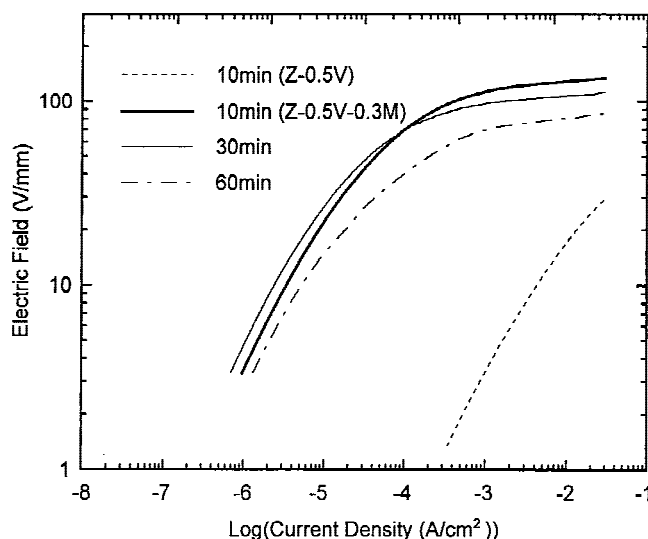
traps, which are, most probably, manganese ions that have partially dissolved into the matrix. By contrast, the manganese species have a tendency to remain at the grain boundaries (i.e., Mn_{gb}), which forms the surface states. Therefore, a reduction in surface-state density (N_s) can occur, because of the partial dissolution of the manganese ions into the grains or the loss of the Mn_{gb} species that accompanies the volatile vanadium species.

Because the proportion of donor (Zn_i) and acceptor (Mn) species that are incorporated in these samples is the same, the only possible reaction that can occur during sintering is a redistribution of these species. Pronounced grain growth that occurs during sintering (cf. Table I) will induce rapid grain-boundary migration. Thus, a significant proportion of manganese ions that had originally resided at the grain boundaries is left behind and dissolved into the grains, which results in a decrease in the value of N_d.

Moreover, a loss of the manganese species through vaporization will occur, in addition to an inward diffusion of the manganese species into the grains, for the samples that have been sintered at high temperature (or for long soaking times).

Such a phenomenon leads to a significant reduction in the value of N_s for samples sintered at 1200°C (for 10 min) and explains the significant degradation of the nonlinear properties of these materials very well.

The above-mentioned discussions clearly indicate that the processing parameters that have been used to sinter the ZnO–V_2O_5–Mn_3O_4 materials markedly modify the defect chemistry along grain boundaries, which significantly alters the nonohmic properties of the materials. This phenomenon occurs mainly via redistribution of the additives.

V. Conclusion

The effect of V_2O_5 and Mn_3O_4 additives on the densification behavior and the grain-growth characteristics of the ZnO materials, and their associated nonohmic properties, were system-
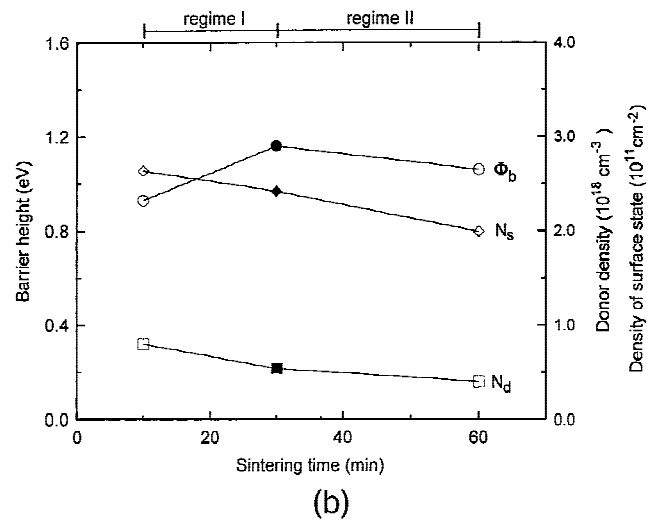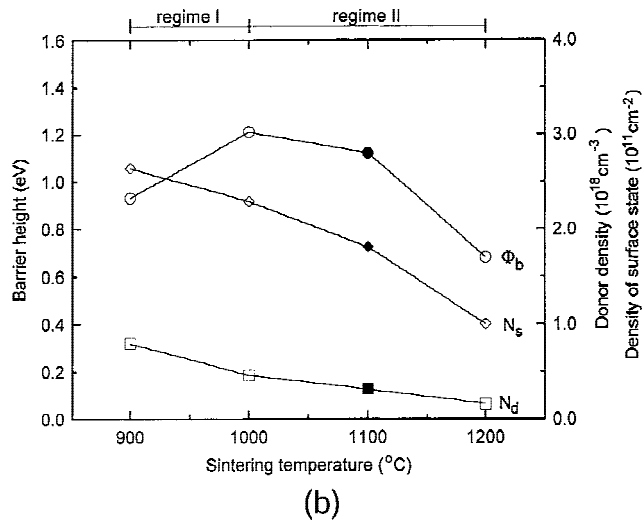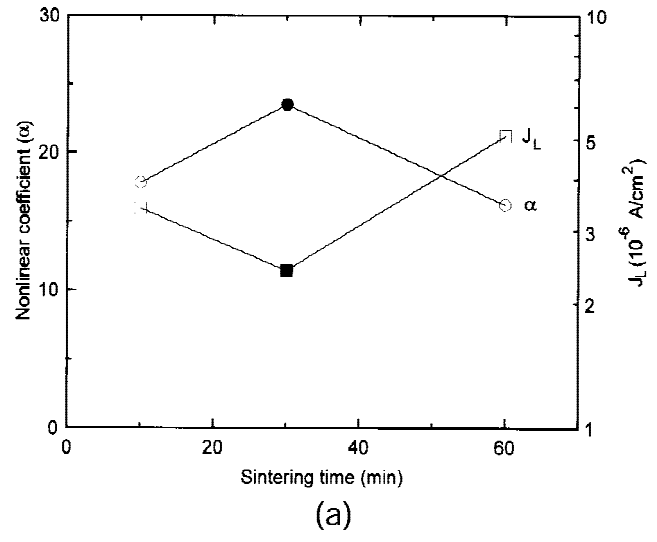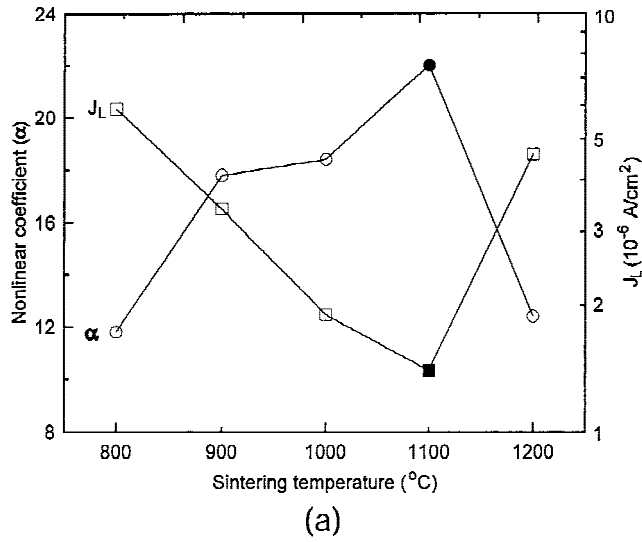
(a)

(a)

(b)

(b)

Fig. 9. Effect of the microwave sintering temperature (800°–1200°C for 10 min) on various properties of ZnO–0.5-mol%-V$_2$O$_5$–0.3-mol%-Mn$_3$O$_4$ materials ((a) (○) the nonlinear coefficient (α) and (□) the leakage current density (J_L); (b) (●) the potential barrier height (Φ_b), (■) the donor density (N_d), and (♦) the surface-state density (N_s)).

Fig. 10. Effect of soaking time (10–60 min for 900°C) on various properties of the ZnO–0.5-mol%-V$_2$O$_5$–0.3-mol%-Mn$_3$O$_4$ materials ((a) (■) nonlinear coefficient (α) and (●) leakage current density (J_L); (b) (●) potential barrier height (Φ_b), (■) donor density (N_d), and (♦) surface-state density (N_s)).

Table I.   Variation of Donor and Surface-State Density (N_d and N_s, Respectively) with Sintering Conditions

Sintering conditions	Grain size (μm)	N_d ($\times 10^{18}$ cm^{-3})	N_s ($\times 10^{11}$ cm^{-2})	α	Φ_b (eV)	Remark
900°C, 10 min	17.9	0.80	2.64	17.8	0.93	
1000°C, 10 min	30.7	0.46[†]	2.29	18.4	1.21	Regime I in Fig. 3[†]
1100°C, 10 min	36.1	0.31	1.81	22.0	1.12	
1200°C, 10 min	44.6	0.16	1.00[‡]	12.4	0.68	Regime II in Fig. 3[‡]
900°C, 10 min	17.9	0.80	2.64	17.8	0.93	
900°C, 30 min	29.7	0.54[†]	2.42	23.5	1.16	Regime I in Fig. 3[†]
900°C, 60 min	32.8	0.40	1.99[‡]	16.2	1.06	Regime II in Fig. 3[‡]

[†]Marked reduction in N_d due to grain growth. [‡]Marked reduction in N_s due to manganese loss.

atically examined. The addition of V$_2$O$_5$ markedly reduced the microwave sintering temperature and soaking time necessary to densify the ZnO materials and induce grain growth. The incorporation of the Mn$_3$O$_4$ species did not significantly modify their sintering properties but did markedly alter their nonohmic behavior. The proper processing parameters, such as the microwave sintering temperature (900°C) and soaking time (30 min), further improved the nonlinear coefficient α and the leak-

age current density J_L through modification of the defect chemistry of the samples.

References

[1]M. Matsuoka, "Nonohmic Properties of Zinc Oxide Ceramics," *Jpn. J. Appl. Phys.*, **10** [6] 736–46 (1971).
[2]M. Inada, "Crystal Phases on Non-ohmic Zinc Oxide Ceramics," *Jpn. J. Appl. Phys.*, **17** [1] 1–10 (1978).

[3]L. M. Levinson and H. R. Philipp, ''Zinc Oxide Varistors—A Review,'' *Am. Ceram. Soc. Bull.*, **65** [4] 639–46 (1986).

[4]T. K. Gupta, ''Application of Zinc Oxide Varistors,'' *J. Am. Ceram. Soc.*, **73** [7] 1817–40 (1990).

[5]K. Eda, A. Iga, and M. Matsuoka, ''Degradation Mechanism of Non-ohmic Zinc Oxide Ceramics,'' *J. Appl. Phys.*, **51** [5] 2678–84 (1980).

[6]J. Erickson and B. Reich, ''The High Power Metal-Oxide Varistor as a Vehicle and Aircraft Transient Suppressor,'' *IEEE Trans. Aerosp. Electron. Syst.*, **AES-12**, 104–108 (1976).

[7]L. M. Levinson and H. R. Philipp, ''ZnO Varistors for Transient Protection,'' *IEEE Trans. Parts, Hybrids, Packag.*, **PHP-13**, 338–43 (1977).

[8]E. C. Sakshaug, J. S. Kresge, and S. A. Miske, ''A New Concept in Station Arrestor Designs,'' *IEEE Trans. Power Appar. Syst.*, **PAS-96**, 647–56 (1977).

[9]R. Einzinger, ''Metal Oxide Varistors,'' *Annu. Rev. Mater. Sci.*, **17**, 299–321 (1987).

[10]J. E. May, ''Properties of 3 Volt Zinc Oxide Varistors''; pp. 295–305 in Ceramic Transactions, Vol. 3, *Advances in Varistor Technology*. Edited by L. M. Levinson, American Ceramic Society, Westerville, OH, 1989.

[11]J. Ozawa, T. Yamazaki, S. Maruyama, S. Shirakawa, A. Mizukoshi, and K. Nakano, ''Applications of Zinc Oxide Nonlinear Elements''; *ibid*, pp. 256–65.

[12]P. Williams, O. L. Krivanek, G. Thomas, and M. Yodogawa, ''Microstructure–Property Relationships of Rare-Earth-Zinc-Oxide Varistors,'' *J. Appl. Phys.*, **51** [7] 3930–34 (1980).

[13]K. Mukae, K. Tsuda, and I. Nagasawa, ''Non-Ohmic Properties of ZnO–Rare Earth Metal Oxide–Co_3O_4 Ceramics,'' *Jpn. J. Appl. Phys.*, **16** [8] 1361–68 (1977).

[14]T. R. N. Kutty and N. Raghu, ''ZnO-Based Voltage-Limiting Resistors with $MCoO_{3-x}$ (M ≡ Ba, Sr) as the Only Forming Additives,'' *Mater. Sci. Eng.*, **B13**, 181–97 (1992).

[15]K. Uematsu, A. Terada, T. Morimoto, N. Uchida, and K. Saito, ''Direct Determination of Grain Growth Behavior in Zinc Oxide with Added Barium Oxide,'' *J. Am. Ceram. Soc.*, **72** [6] 1070–72 (1989).

[16]Y.-S. Lee and T.-Y. Tseng, ''Phase Indentation and Electrical Properties in ZnO–Glass Varistors,'' *J. Am. Ceram. Soc.*, **75** [6] 1636–40 (1992).

[17]G. E. Pike, S. R. Kurtz, P. L. Gourley, H. R. Philipp, and L. M. Levinson, ''Electroluminescence in ZnO-Varistors,'' *J. Appl. Phys.*, **57** [12] 5512–18 (1985).

[18]F. Greuter, G. Blatter, M. Rossinelli, and F. Stucki, ''Conduction Mechanism in ZnO-Varistors: An Overview''; see Ref. 10, pp. 31–53.

[19]J. K. Tsai and T. B. Wu, ''Non-Ohmic Characteristics of $ZnO–V_2O_5$ Ceramics,'' *J. Appl. Phys.*, **76** [8] 4817–22 (1994).

[20]W. H. Sutton, ''Microwave Processing of Ceramic Materials,'' *Am. Ceram. Soc. Bull.*, **68** [2] 376–86 (1989).

[21]M. A. Janney, C. L. Calhoun, and H. D. Kimery, ''Microwave Sintering of Solid Oxide Fuel Cell Materials: I. Zirconia–8 mol% Yttria,'' *J. Am. Ceram. Soc.*, **75** [2] 341–46 (1992).

[22]H. Y. Chang, K. S. Liu, and I. N. Lin, ''Electrical Characteristics of $(Sr_{0.2}Ba_{0.8})TiO_3$ Positive Temperature Coefficient of Resistivity Materials Prepared by Microwave Sintering,'' *J. Appl Phys.*, **77** [11] 1–5 (1995).

[23]C. S. Chen, C. T. Kuo, and I. N. Lin, ''Electrical Properties of ZnO Varistors Prepared by Microwave Sintering Process,'' *Jpn. J. Appl. Phys.*, **35** [9] 4696–703 (1996).

[24]C. T. Kuo, C. S. Chen, and I. N. Lin, ''Microstructure and Nonlinear Properties of Microwave-Sintered $ZnO–V_2O_5$ Varistor: I, Effect of V_2O_5 Doping,'' *J. Am. Ceram. Soc.*, **81** [11] 2942–48 (1998).

[25]M. I. Mendelson, ''Average Grain Size in Polycrystalline Ceramics,'' *J. Am. Ceram. Soc.*, **52** [8] 443–46 (1969).

[26]K. Mukae, K. Tsuda, and I. Nagasawa, ''Capacitance-vs-Voltage Characteristics of ZnO Varistors,'' *J. Appl. Phys.*, **50** [6] 4475–76 (1979).   □